Proceedings of Anticancer Research, 2026, Volume 10, Issue 4
http://ojs.bbwpublisher.com/index.php/PAR
Online ISSN: 2208-3553
Print ISSN: 2208-3545

# Transcriptomic Analysis of Organ-Specific Metastasis Regulation in Breast Cancer

**Jiayin Wang[1], Qiushuang Ma[1], Bingjuan Zhou[1], Jirui Sun[1], Zhihong Li[2], Haizhi Qiao[1], Xueli Wang[1], Jinku Zhang[1]**

[1]Department of Pathology, Key Laboratory of Molecular Pathology and Early Diagnosis of Tumor in Hebei Province, Baoding NO.1 Central Hospital, Baoding 071000, Hebei, China
[2]Baoding NO.1 Hospital, Baoding 071000, Hebei, China



**Abstract:** *Objective:* This study aimed to investigate the underlying mechanisms of breast cancer metastasis patterns through a transcriptomic analysis of breast cancer with organ-specific metastasis. *Methods:* (1) Breast cancer cell lines capable of specific lung and bone metastasis were constructed using the PyMT-1 cell line. (2) The IVIS imaging system was employed to screen cell lines with robust specific metastatic capabilities. (3) Transcriptome sequencing was conducted on the resultant breast cancer cell lines exhibiting specific metastasis. (4) The transcriptome sequencing data were analyzed to identify pathways influencing specific metastasis in breast cancer. (5) Validation of pathway-related genes through PCR detection. (6) Clinical validation of differentially expressed genes in paraffin specimens. *Results:* (1) The IVIS system confirmed the specific metastatic abilities of PyMT-1, Py-L1, Py-L2, Py-B1 and Py-B2 tumors. PyMT-1, Py-L1 and Py-B1 were chosen for further experiments. (2) Following transcriptome sequencing, differentially expressed genes were identified and enrichment analysis was conducted. Pairwise comparisons among the three cell lines revealed 917 differentially expressed genes between PyMT-1 and Py-L1 (including 641 upregulated and 276 downregulated genes); 4131 differentially expressed genes between PyMT-1 and Py-B1 (including 2158 upregulated and 1973 downregulated genes). *Conclusions:* This study analyzed the genetic background related to breast cancer-specific lung and bone metastasis at the transcriptome level. Obtained the corresponding differential expression profiles and potential functional pathways involved. Demonstrated the promoting roles of CCN2 and ITGB6 in breast cancer lung metastasis, and the promoting roles of CD44 and THBS1 in breast cancer bone metastasis.

**Keywords:** Breast cancer; Specific metastasis; Transcriptome sequencing

**Online publication:** August 11, 2026

## 1. Introduction

According to the epidemiological data statistics on various types of cancer released by the International Agency for Research on Cancer (IARC) under the World Health Organization in April 2024, breast cancer

(with an incidence rate of 11.6%) is the most common cancer among women and the fourth leading cause of cancer-related deaths. The incidence of breast cancer among Chinese women is increasing year by year [1]. According to the latest statistics, the age-standardized incidence rate of breast cancer in China is 39.10 per 100, 000 [2]. Compared to the past, with improvements in early diagnosis and treatment of breast cancer, the disease-free survival period and overall survival period of patients have significantly increased. Although the mortality rate of cancer has decreased [3], the incidence of breast cancer is on the rise, with distant metastasis being the primary cause of high mortality in breast cancer patients, accounting for over 90% of cancer deaths due to metastasis of breast cancer.

Due to the current poor efficacy of metastatic breast cancer treatment and the lack of early prediction methods to determine which organs are prone to metastasis, patients with metastatic breast cancer often have a poor prognosis. Therefore, exploring the mechanisms driving breast cancer-specific metastasis is of great significance for identifying new biomarkers and therapeutic targets.

## 2. Materials and methods

### 2.1. Experimental materials

PPyMT-1, Py-L1, Py-L2, Py-B1, and Py-B2 cells were obtained from the School of Translational Medicine, Zhejiang University. Female C57BL/6 mice aged 8 weeks were purchased from Jiangsu Jicui Kang Biotechnology Co., Ltd., with an experimental animal production license number: SCXK (Su) 2018-0008. The experimental protocol was approved by the Experimental Animal Ethics Committee of the First Affiliated Hospital, Zhejiang University School of Medicine, with ethics approval number: (2024) Experimental Animal Fast Review No. (687).

With the approval of the ethics committee, clinical and pathological information from 38 patients with invasive ductal carcinoma (IDC) at Baoding First Central Hospital from 2016 to 2023 was collected, with ages ranging from 30 to 68 years and an average age of 51.6 years. Paraffin-embedded tissues included both adjacent and cancerous tissues: 25 cases without distant metastasis, 7 cases with lung metastasis, and 6 cases with bone metastasis. All sections were reviewed and verified by two senior pathologists according to the latest edition of the “WHO Classification of Tumours of the Breast.”

### 2.2. Acquisition of Py-L1, Py-L2, Py-B1, and Py-B2 tumor cells

In vitro cultured and amplified PyMT-1 tumor cells were inoculated into immunodeficient mice (nude mice): cell lines capable of lung metastasis (Py-L1, Py-L2) were screened through tail vein injection, and cell lines capable of bone metastasis (Py-B1, Py-B2) were screened through left ventricular injection. The tumor-specific metastatic ability of Py-L1, Py-L2, Py-B1, and Py-B2 cells was verified using the IVIS system. Groups with better tumor formation were selected for subsequent experiments.

### 2.3. Transcriptome sequencing of Py-L1, Py-L2, Py-B1, and Py-B2 tumor cells

Total RNA was extracted from Py-L1, Py-L2, Py-B1, and Py-B2 tumor cells for sequencing and information analysis. The acquired whole transcriptome expression files required processing steps such as raw data filtering, sequencing error rate checking, and GC content distribution checking, with the final data summarized.

## 2.4. Transcriptome data analysis

### 2.4.1. Differential gene screening

First, genes were filtered based on the mean count values, retaining only those with mean counts > 2 in each group for subsequent analysis. The R package DESeq2 was used to normalize the count data across all samples and to calculate the fold changes. Differential expression between the two groups was then statistically tested. Finally, protein-coding genes were selected as differentially expressed based on the fold change and significance test results. In this study, the screening criteria were defined as adjusted *P*-value (q-value) < 0.05 and $|\log_2(\text{fold change})| > 0.5$. The differentially expressed genes were visualized using volcano plots and heatmaps.

### 2.4.2. Functional analysis of differential genes

ClusterProfiler software was used to perform GO enrichment analysis and functional annotation of differential genes to investigate the biological roles of significantly differentially expressed genes in the study. KEGG pathway analysis was also conducted to identify the most important pathways with significant changes in the study samples. The differential gene set consisted of genes that were significantly differentially expressed and annotated to the GO or KEGG databases, while the background gene set consisted of all genes subjected to significant differential analysis. To assess pathway differences among different subsets, Gene Set Enrichment Analysis (GSEA) was also performed.

## 2.5. Validation of differentially expressed genes

The qPCR method was used to validate the expression of differential genes in cell wax blocks from 38 patients at Baoding First Central Hospital.

# 3. Results

## 3.1. Validation of cell metastatic ability

PyMT-1, Py-L1, Py-L2, Py-B1, and Py-B2 cell lines were injected into mice via tail vein injection, and the growth of cancer foci in mice was observed at 7, 14, 21, and 28 days. The results showed that the fluorescence signal intensity and range at the tumor formation sites in mice in the Py-L1 and Py-B1 groups were significantly higher than those in the Py-L2 and Py-B2 groups (**Figure 1**). Therefore, Py-L1 and Py-B1 were used as breast cancer-specific metastatic cell lines for subsequent transcriptomic analysis in subsequent experiments.

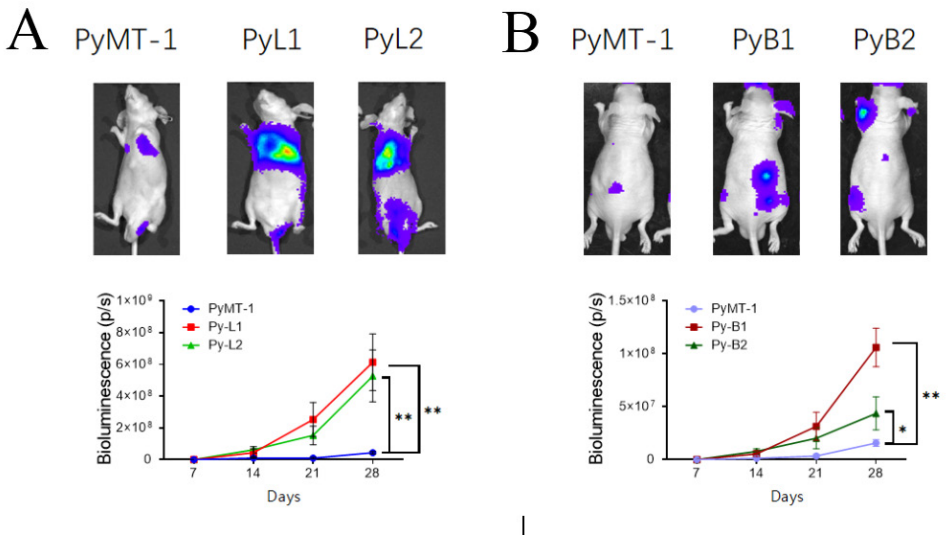


**Figure 1.** Verification of the metastatic ability of Py-L1 and Py-B1 cells.*indicates $P < 0.05$, ** indicates $P < 0.01$.

## 3.2. Transcriptome analysis results of PyMT-1, Py-L1, and Py-B1

### 3.2.1. Transcriptome data analysis results and validation of PyMT-1 and Py-L1

#### 3.2.1.1. Analysis of differentially expressed genes

In this study, the DESeq2 R package (v3.6.1) was used to analyze differentially expressed genes from the quality-controlled transcriptome data. A total of 917 differentially expressed genes were identified, including 641 upregulated genes and 276 downregulated genes. The visual volcanic plot is presented below (**Figure 2**).

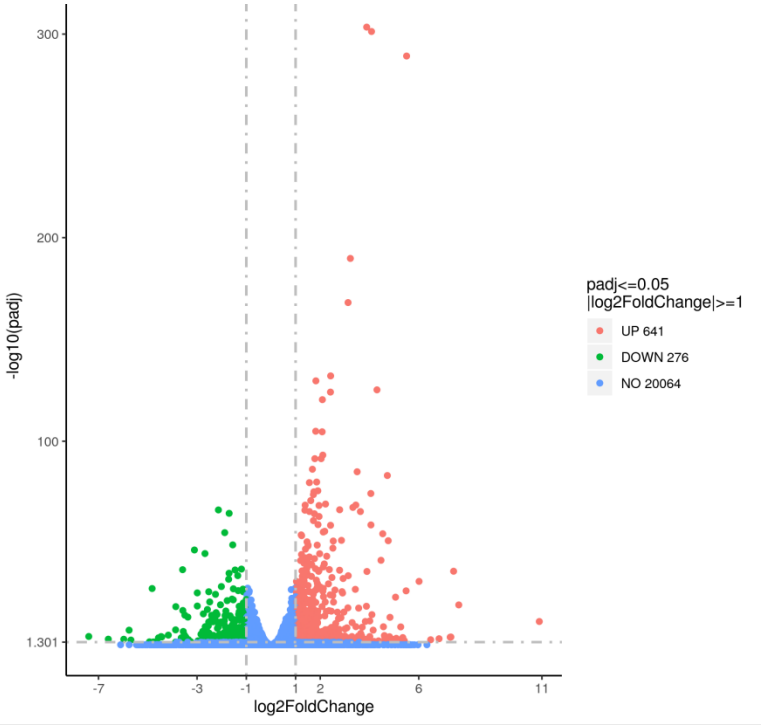


**Figure 2.** Volcano plot of differentially expressed genes between PyMT-1 and Py-L1.

### 3.2.1.2. Enrichment analysis of differentially expressed protein-coding RNAs

As mentioned earlier, a total of 917 differentially expressed protein-coding RNAs were identified between the PyMT-1 and Py-L1 groups. GO, KEGG enrichment analyses, and GSEA were performed on the differential gene sets.

#### 3.2.1.2.1. Results of GO functional enrichment analysis

After screening for differentially expressed genes, GO functional enrichment analysis was performed and described from three aspects: biological process (BP), cellular component (CC), and molecular function (MF). A threshold of $P < 0.05$ was used to identify significantly enriched GO terms. The enrichment results were visualized as bubble plots, as shown in **Figure 3**.

Compared with PyMT-1 cells, the upregulated (**Figure 3A**) and downregulated (Figure 3B) GO pathways in Py-L1 cells are presented. The x-axis represents GeneRatio, defined as the number of genes enriched in a specific pathway divided by the total number of genes in the input gene set. The y-axis represents the specific biological pathways. The size of each bubble indicates the gene count (i.e., the number of genes enriched in the GO term), with larger bubbles representing more genes. The color of each bubble represents the significance of the pathway, expressed as the negative logarithm of the $P$ value ($-\log_{10}(P \text{ value})$), with redder bubbles indicating more significant $P$ values.

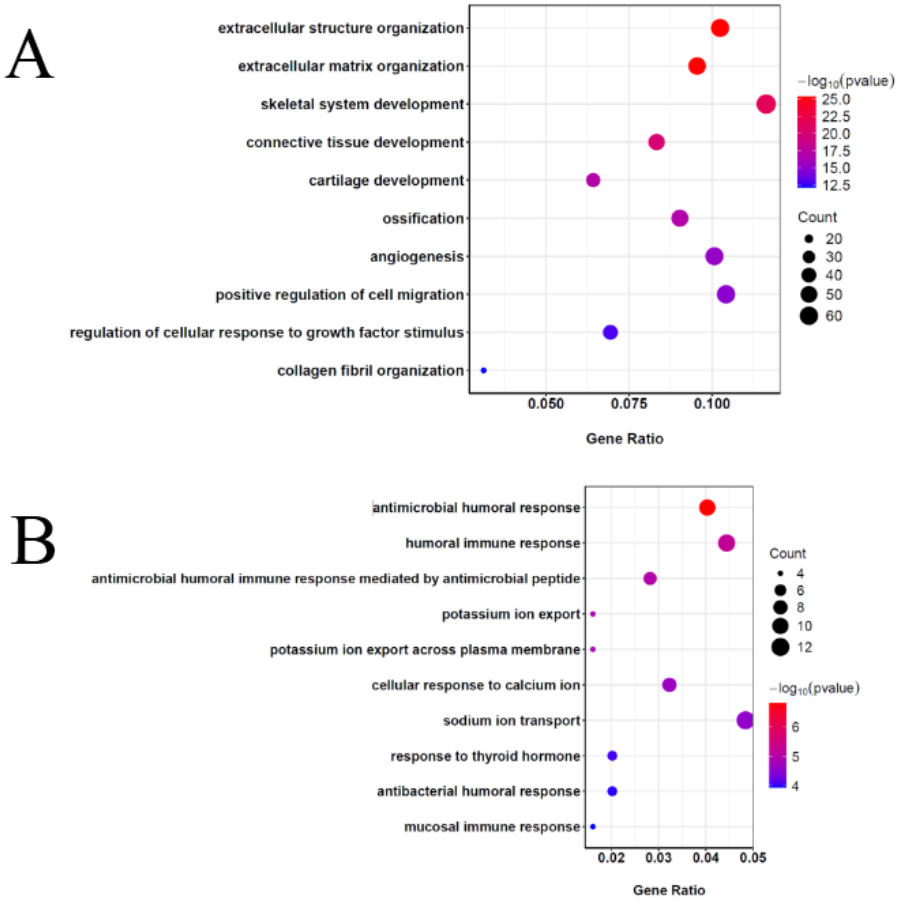


**Figure 3.** GO pathway analysis of differential genes in PyMT-1 and Py-L1 cells.

### 3.2.1.2.2. Results of KEGG pathway enrichment analysis

KEGG is a comprehensive database that integrates genomic, chemical, and systemic functional information. KEGG [4] pathway enrichment analysis can identify significantly affected metabolic and signal transduction pathways. A significance enrichment threshold of $P < 0.05$ was used for KEGG pathway enrichment, and the top 10 significantly enriched pathways were selected. The visualization of the enrichment results in a bubble plot is shown below (**Figure 4**).

Compared to PyMT-1, the KEGG pathways that are upregulated (**Figure 4A**) and downregulated (**Figure 4B**) in Py-L1 cells are depicted; the x-axis represents the ratio of the number of differentially expressed genes annotated to the KEGG pathway to the total number of differentially expressed genes, while the y-axis represents the KEGG pathways. The size of the bubbles indicates the number of genes enriched in the KEGG pathway.

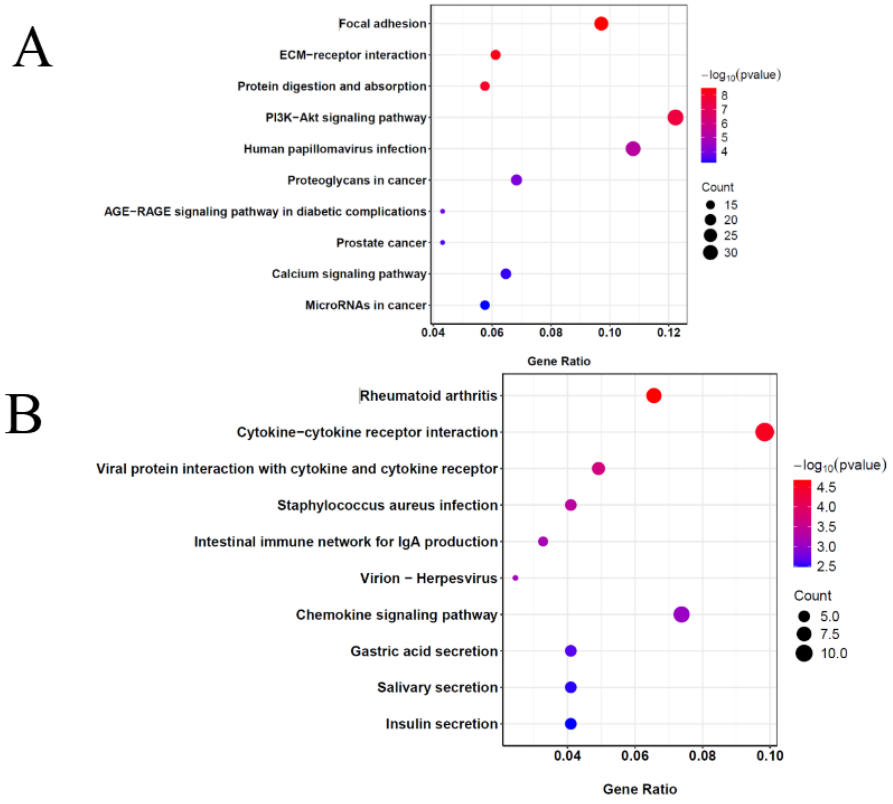


**Figure 4.** KEGG pathway analysis of differential genes in PyMT-1 and Py-L1 cells.

Based on the aforementioned pathway analysis, it can be observed that the differential genes between PyMT-1 and Py-L1 are primarily associated with cellular activities such as extracellular structural organization, extracellular matrix, as well as signaling pathways including PI3K-Akt, focal adhesion, and ECM-receptor interactions.

GO functional enrichment analysis of the differential genes revealed that among the genes upregulated in Py-L1, the most representative functional genes are primarily involved in biological processes such as extracellular matrix organization (ECM), skeletal system development, connective tissue development, positive regulation of cell migration, and angiogenesis. Conversely, the downregulated genes are mainly

associated with processes such as antimicrobial humoral response, antimicrobial peptide-mediated humoral immune response, humoral immune response, sodium-potassium-calcium ion transport, and mucosal immune response.

In KEGG pathway enrichment analysis, the upregulated differential genes were primarily associated with pathways such as focal adhesion (an important connection point between cells and the extracellular matrix, involved in signal transduction and processes like cell migration and growth), ECM-receptor interaction (the interaction between the extracellular matrix and cell surface receptors is crucial for cell adhesion, migration, and signal transduction), protein digestion and absorption, PI3K-Akt signaling pathway, human papillomavirus infection, cancer-associated proteoglycans, and calcium signaling pathway. The downregulated differential genes were mainly associated with pathways such as cytokine-cytokine receptor interaction, Staphylococcus aureus infection, herpesvirus infection, and chemokine signaling pathway.

### 3.2.1.2.3. Pathways upregulated in Py-L1 cells as revealed by GSEA analysis

GSEA analysis results indicated that the differentially expressed genes were primarily enriched in pathways related to extracellular tissue structure and connective tissue development (**Figure 5**).

When analyzing the enrichment degree of gene sets, the peak of the ES (Enrichment Score) can be observed. The peak of the green curve reflects the maximum enrichment degree of the gene set. A positive peak indicates a positive enrichment of gene sets related to extracellular tissue structure and connective tissue development in Py-L1 cells, with the core genes of the relevant pathways being those preceding the peak.

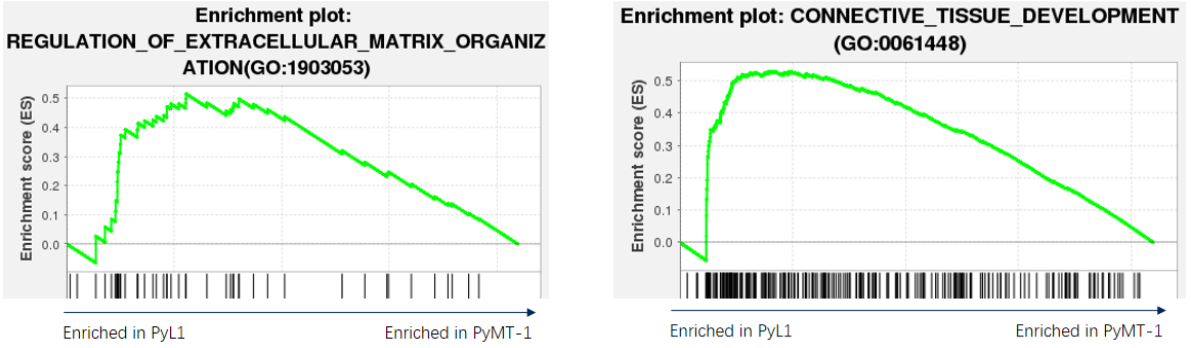


**Figure 5.** Up-regulated pathways in Py-L1 cells compared to PyMT-1.

### 3.2.1.3. Real-time fluorescent quantitative PCR detection of differential gene expression levels in PyMT-1 and Py-L1

To further validate the transcriptional levels of genes related to the ECM-receptor interaction and cytokine-cytokine receptor interaction pathways in breast cancer-specific lung metastasis, qPCR experimental techniques were employed to detect differences in the transcriptional levels of genes associated with these two pathways in PyMT-1 and Py-L1. The results are as follows (**Figure 6**). In **Figure 6A**, compared to PyMT-1, the expression levels of genes related to the ECM-receptor interaction pathway, namely Cellular Communication Network Factor 2 (CCN2), COL1A1, and ITGB6, were all elevated in the Py-L1 cell line. In Figure 6B, compared to PyMT-1, the expression levels of genes related to cytokine-cytokine receptor interaction, namely CXCL5, TNF, and CXCR4, were all decreased in the Py-L1 cell line.

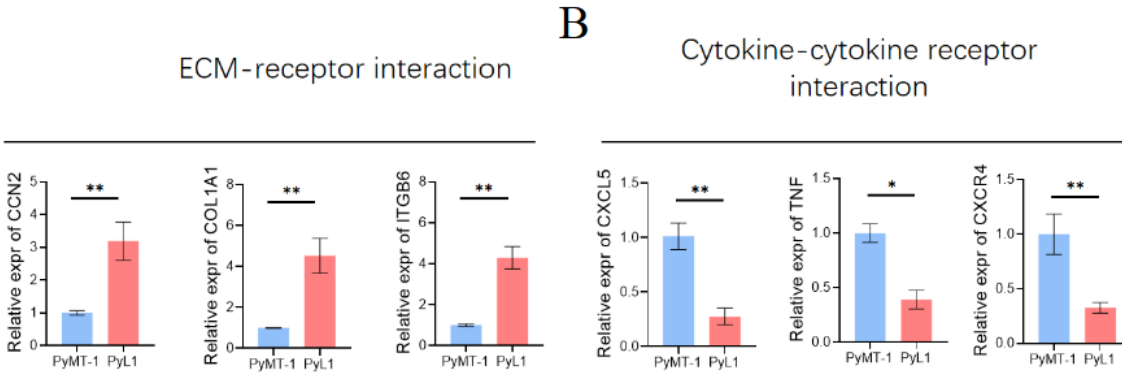


**Figure 6.** PCR validation results of up-regulated and down-regulated pathways in Py-L1 cell lines compared with PyMT-1.*indicates $P < 0.05$, ** indicates $P < 0.01$.

### 3.2.1.4. Clinical validation of differentially expressed genes

Among the 38 cases of IDC tissues, the significantly highly expressed genes CCN2 and ITGB6 identified in Py-L1 cells were validated. The results are as follows (Figure 7): Compared to breast cancer tissues without metastasis, the expression levels of the lung-specific metastatic genes CCN2 and ITGB6 were significantly elevated in breast cancer tissues with lung metastasis ($P < 0.05$), while there was no significant change in their expression levels in breast cancer tissues with bone metastasis.

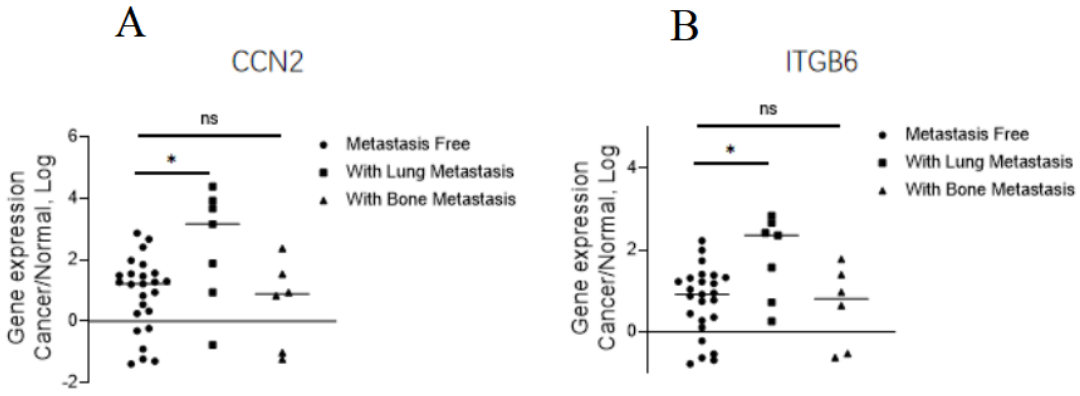


**Figure 7.** The expression levels of CCN2 and ITGB6 are elevated in breast cancer with lung metastasis.*indicates $P < 0.05$, and ns indicates no statistical difference.

### 3.2.2. Results and validation of transcriptome data analysis for PyMT-1 and Py-B1

### 3.2.2.1. Analysis of differentially expressed genes

A total of 4, 131 differentially expressed genes were identified, including 2, 158 upregulated genes and 1, 973 downregulated genes. The visualized volcano plot is shown below (**Figure 8**).

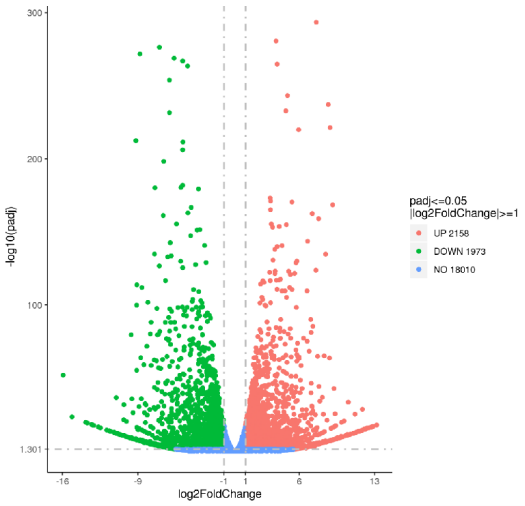


**Figure 8.** Volcano plot of differentially expressed genes between PyMT-1 and Py-B1.

### 3.2.2.2. Enrichment analysis of differentially expressed protein-coding RNAs

As previously mentioned, a total of 4, 131 differentially expressed protein-coding RNAs were identified between the PyMT-1 and Py-B1 groups. GO, KEGG pathway enrichment analysis, and GSEA analysis were performed on the set of differentially expressed genes.

#### 3.2.2.2.1. Results of GO functional enrichment analysis

After screening the differentially expressed genes, the visualized bubble plot of the GO functional enrichment analysis results is shown below (**Figure 9**).

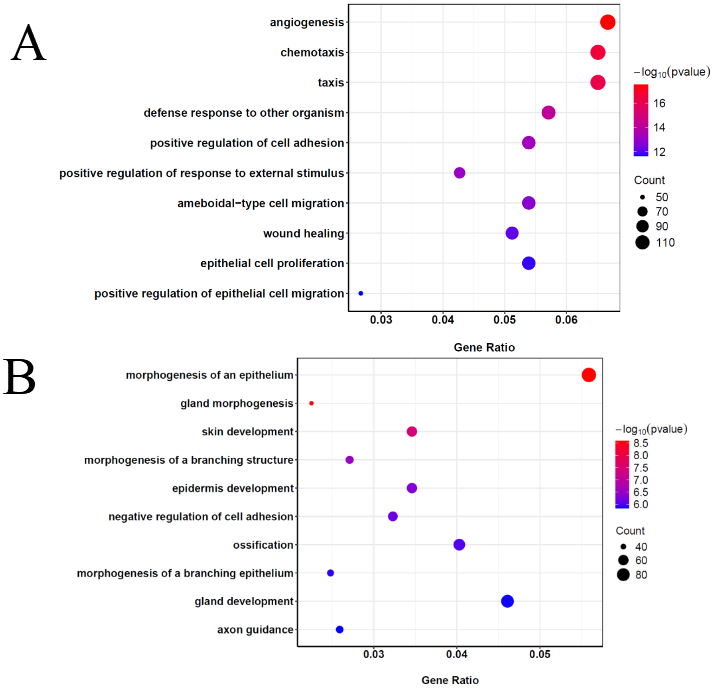


**Figure 9.** GO pathway analysis of differential genes in PyMT-1 and Py-B1 cells.

### 3.2.2.2.2. Results of KEGG pathway enrichment analysis

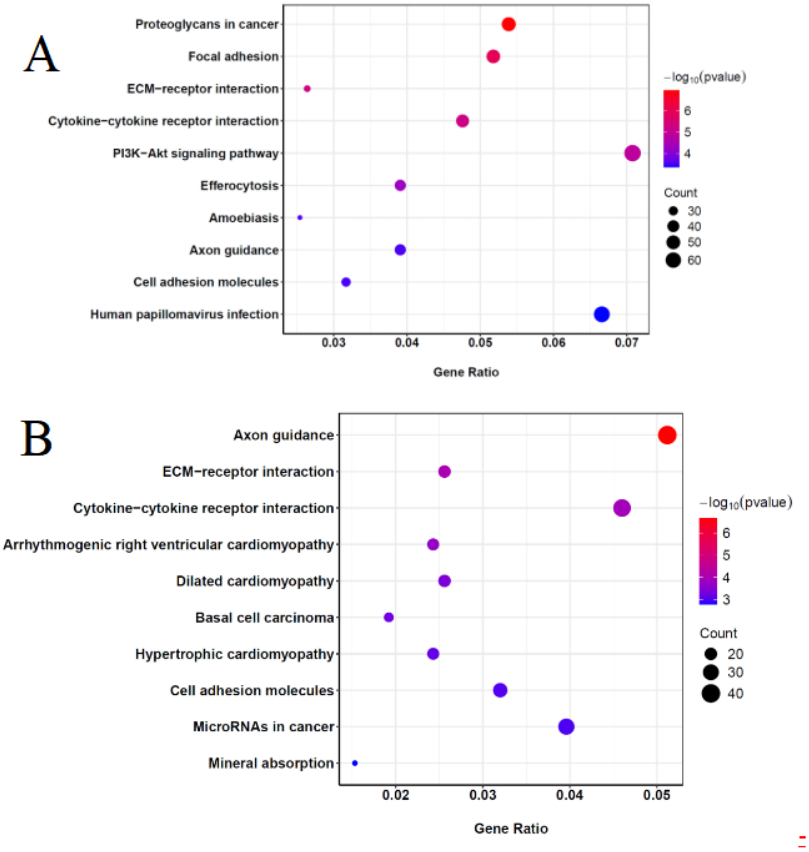


**Figure 10.** KEGG pathway analysis of differential genes in PyMT-1 and Py-B1 cells.

Through the aforementioned pathway analysis, it can be observed that the differentially expressed genes between PyMT-1 and Py-B1 are primarily associated with cellular activities such as angiogenesis, chemotaxis, positive regulation of cell adhesion, epithelial cell proliferation, and positive regulation of epithelial cell migration, as well as pathways including proteoglycans in cancer, focal adhesion, ECM-receptor interaction, cytokine-cytokine receptor interaction, and the PI3K-Akt signaling pathway.

GO functional enrichment analysis of the differentially expressed genes revealed that among the genes upregulated in Py-B1, the most representative functional genes are primarily involved in biological processes such as angiogenesis, chemotaxis, positive regulation of cell adhesion, epithelial cell proliferation, and positive regulation of epithelial cell migration. Conversely, the downregulated genes are mainly associated with processes such as epithelial morphogenesis, gland morphogenesis, negative regulation of cell adhesion, ossification, and axon guidance.

In KEGG pathway enrichment analysis, the upregulated differentially expressed genes are primarily related to pathways such as proteoglycans in cancer, focal adhesion, ECM-receptor interaction, cytokine-cytokine receptor interaction, PI3K-Akt signaling pathway, efferocytosis, axon guidance, and cell adhesion molecules. The downregulated differentially expressed genes are mainly associated with pathways such as synaptic guidance, ECM-receptor interaction, cytokine-cytokine receptor interaction, cell adhesion

molecules, and microRNAs in cancer.

### 3.2.2.2.3. Pathways upregulated in Py-B1 cells as revealed by GSEA analysis

GSEA analysis results indicate that the differentially expressed genes are primarily enriched in pathways related to embryonic skeletal system development and fibroblast growth response (**Figure 11**).

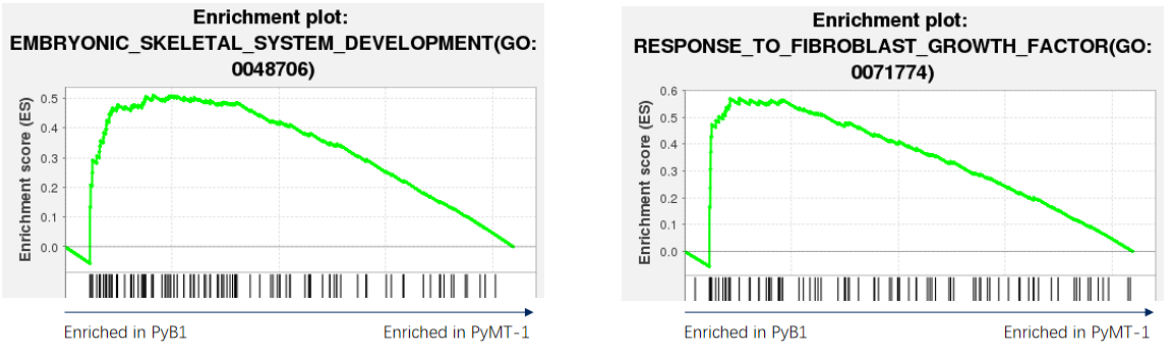


**Figure 11.** Up-regulated pathways in Py-B1 cells compared to PyMT-1.

### 3.2.2.3. Real-time fluorescent quantitative PCR analysis of differential gene expression levels in PyMT-1 and Py-B1

To further validate the expression levels of genes related to the proteoglycans in cancer and miRNA pathways in cancer, specifically in the context of breast cancer-specific bone metastasis, qPCR experimental techniques were employed to detect the transcriptional differences of genes associated with these two pathways in PyMT-1 and Py-B1. The results are presented as follows (**Figure 12**). In **Figure 12A**, compared to PyMT-1, the expression levels of genes related to the upregulated proteoglycans in cancer pathway, namely CD44, THBS1, and CAV1, are all elevated in the Py-B1 cell line. In **Figure 12B**, compared to PyMT-1, the expression levels of genes related to the downregulated miRNA pathway in cancer, specifically ST14, DNMT3A, and DNMT3B, are all decreased in the Py-B1 cell line.

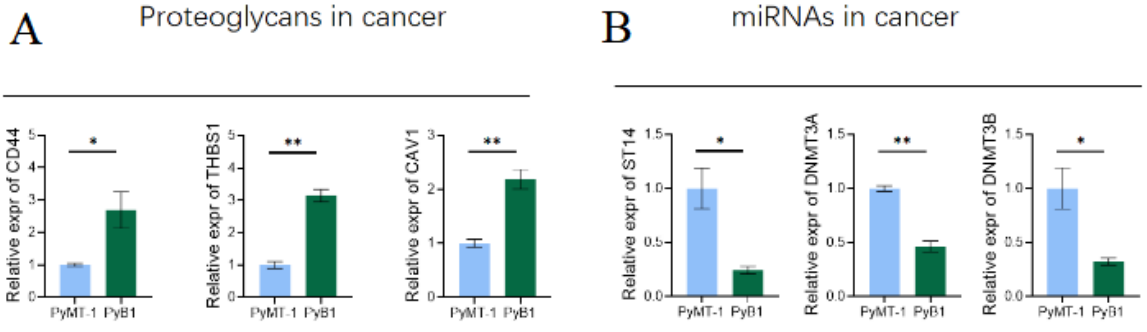


**Figure 12.** PCR validation results of up-regulated and down-regulated pathways in Py-B1 cell lines compared with PyMT-1.*indicates $P < 0.05$, ** indicates $P < 0.01$.

### 3.2.2.4. Clinical validation of differentially expressed genes

In 38 cases of invasive ductal carcinoma (IDC) tissues, the significantly highly expressed genes CD44 and

THBS1 identified in Py-B1 cells were validated. The results are as follows (**Figure 13**): Compared to breast cancer tissues without metastasis, the expression levels of the bone-specific metastasis genes CD44 and THBS1 were elevated in breast cancer tissues with bone metastasis ($P < 0.05$), while their expression levels remained unchanged in breast cancer tissues with lung metastasis.

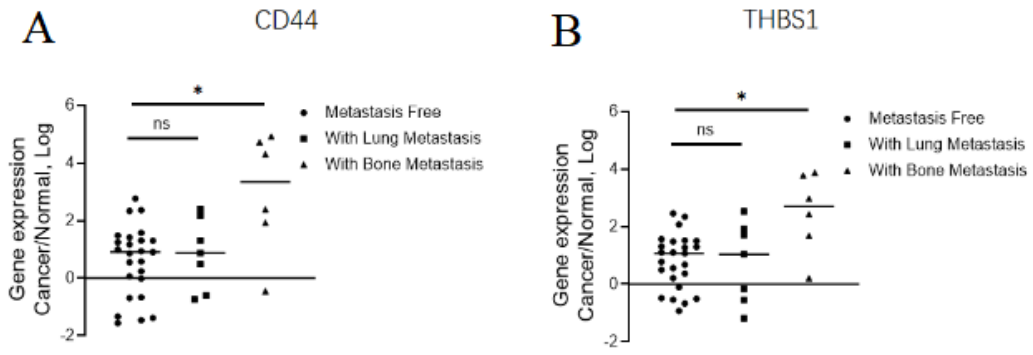


**Figure 13.** The expression levels of CD44 and THBS1 are elevated in breast cancer with bone metastasis.*indicates $P < 0.05$, ns indicates no statistical difference.

## 4. Discussion

According to the epidemiological data statistics for various types of cancer released by the International Agency for Research on Cancer (IARC) in April 2024, breast cancer stands as the most prevalent cancer among women and ranks fourth as a cause of cancer-related deaths. Distant metastasis is the primary contributor to the high mortality rate associated with breast cancer, with over 90% of cancer deaths attributed to metastatic spread. The expression of specific molecular mediators at both primary and metastatic sites determines the propensity of tumor cells to metastasize to particular target organs. Breast cancer exhibits metastatic heterogeneity, favoring different organs. Recent studies have identified bone, lung, and liver as common sites for distant metastasis in breast cancer, a phenomenon termed organ-specific metastasis. This study focuses on mouse models of breast cancer with specific bone and lung metastases, employing transcriptomic analysis to explore the underlying mechanisms of breast cancer-specific metastasis.

The efficiency of the metastatic process is exceedingly low, with less than 0.01% of tumor cells from the primary tumor capable of completing distant metastasis and forming secondary lesions at distant sites [5]. Clinically established patterns of organ-specific metastasis indicate that the sites of distant metastasis are not random but are influenced by the microenvironment of the target organ.

### 4.1. Biological function analysis of coding genes related to PyMT-1 and Py-L1

By comparing the PyMT-1 and Py-L1 cell lines, we identified differential genes potentially associated with lung metastasis in breast cancer. Enrichment analysis revealed relevant signaling pathways regulating lung metastasis in breast cancer.

Based on previous results, a total of 917 differential genes were identified between PyMT-1 and Py-L1, including 641 upregulated and 276 downregulated genes. These differential genes underwent GO functional enrichment analysis, KEGG pathway enrichment analysis, and GSEA analysis. Pathway enrichment analysis

indicated that the differential genes were primarily associated with cellular activities such as extracellular structure organization, ECM, skeletal development system, connective tissue development, and angiogenesis, as well as pathways like focal adhesion, PI3K-Akt signaling pathway, and ECM-receptor interaction. The activation or alteration of these pathways suggests their potential involvement in the specific lung metastasis of breast cancer.

Subsequent PCR validation confirmed the upregulation of genes related to ECM-receptor interaction in the upregulated pathway, namely CCN2, COL1A1, and ITGB6, which were significantly elevated in Py-L1 compared to PyMT-1 cell lines. Conversely, genes associated with cytokine-cytokine receptor interaction in the downregulated pathway, such as CXCL5, TNF, and CXCR4, were downregulated in Py-L1. Further validation in clinical samples demonstrated significantly elevated expression levels of CCN2 and ITGB6 in breast cancer tissues with lung metastasis, with no significant changes observed in IDC tissues without metastasis or with bone metastasis. This further suggests that CCN2 and ITGB6 may promote specific lung metastasis in IDC.

The crucial regulatory role of ECM in breast cancer has been widely acknowledged. Compared to normal breast tissue, ECM undergoes significant changes in composition and organization during breast cancer progression. Studies have shown that proteomic analysis of ECM in breast tumors of xenograft mouse models reveals distinct ECM compositions between tumors with high and low metastatic potential [6]. Current research on ECM in breast cancer metastasis is relatively thorough. For instance, Tenascin C (TNC), a cellular matrix protein in ECM, interacts with cell surface receptors and ECM proteins. In the breast, TNC expression is associated with mammary gland involution and breast cancer development [7]. In breast cancer cells, TNC is regulated by microRNA miR335 [8, 9]. Metastatic breast cancer cells with a high propensity for lung metastasis often exhibit a loss of miR335 expression, leading to TNC upregulation. The mechanism may involve TNC sequentially activating macrophages and endothelial cells and generating a pro-metastatic vascular niche in the lungs [10]. Therefore, TNC from different sources in the tumor microenvironment promotes the metastatic progression of breast cancer, a finding further validated by this study. Simultaneously, inhibiting ECM components that promote tumor progression and metastasis may represent an effective strategy for treating breast cancer.

CCN2 regulates key biological activities such as cell growth, invasion, and migration. It modulates the breast tumor microenvironment by promoting angiogenesis, activating cancer-associated fibroblasts (CAFs), and inducing inflammation. The activity of CCN2 depends on various factors and varies by breast cancer type. This factor has been shown to promote tumor progression by activating multiple signaling pathways in breast cancer and regulating the expression of genes that facilitate migration, invasion, and chemotherapy resistance. Studies indicate that CCN2 can promote the expression of glucose transporter 3 (GLUT3), facilitating cell survival and metabolism, and upregulate VEGF expression to drive angiogenesis, supporting tumor growth [11,12]. This study found that CCN2 expression was upregulated only in IDC with lung metastasis, suggesting its potential as a specific lung metastasis marker.

The pre-metastatic niche (PMN) generated by primary tumors in specific target organs is crucial for the subsequent colonization and metastasis of tumor cells, involving vascular permeability and angiogenesis, immunosuppression, inflammation, and organ specificity [13]. The initial stage of PMN formation is characterized by angiogenesis and vascular permeability. Several PMN biomarkers related to angiogenesis and vascular permeability have been reported to aid in the diagnosis and treatment of metastatic cancer.

For example, cancer-associated fibroblasts (CAFs) are the primary stromal component of the tumor microenvironment [14]. CAFs not only promote cancer growth and metastasis by secreting cytokines and exosomes and synthesizing and remodeling the extracellular matrix [15,16] but also play a major role in angiogenesis by secreting cytokines [17,18]. AKT is a key factor in the PI3K-Akt signaling pathway. Three different AKT isoforms, namely AKT1, AKT2, and AKT3, are currently known. The PI3K-Akt signaling pathway is frequently altered in breast cancer patients. AKT typically promotes proliferation by regulating the cell cycle and prevents apoptosis by inhibiting pro-apoptotic proteins and promoting anti-apoptotic signals. Some studies have confirmed the anti-metastatic and anti-migratory abilities of AKT1, independent of breast cancer subtype [19,20].

## 4.2. Biological function analysis of coding genes related to PyMT-1 and Py-B1

By comparing the PyMT-1 and Py-B1 cell lines, we identified differential genes potentially associated with bone metastasis in breast cancer. Enrichment analysis revealed relevant signaling pathways regulating bone metastasis in breast cancer.

Based on previous results, a total of 4131 differential genes were identified between PyMT-1 and Py-B1, including 2158 upregulated and 1973 downregulated genes. These differential genes underwent GO functional enrichment analysis, KEGG pathway enrichment analysis, and GSEA analysis. Pathway enrichment analysis indicated that the differential genes were primarily associated with cellular activities such as angiogenesis, chemotaxis, positive regulation of cell adhesion, epithelial cell proliferation, and positive regulation of epithelial cell migration, as well as pathways like proteoglycans in cancer, focal adhesion, ECM-receptor interaction, cytokine-cytokine receptor interaction, and PI3K-Akt signaling pathway. Genes with altered expression levels in these two cell lines may be correlated with specific bone metastasis in breast cancer.

Subsequent PCR validation confirmed the upregulation of genes related to proteoglycans in cancer in the upregulated pathway, namely CD44, THBS1, and CAV1, which were significantly elevated in Py-B1 compared to PyMT-1 cell lines. Conversely, genes related to miRNA function in cancer in the downregulated pathway, such as ST14, DNMT3A, and DNMT3B, were downregulated in Py-B1. Further validation in clinical samples demonstrated significantly elevated expression levels of CD44 and THBS1 in breast cancer tissues with bone metastasis, with no significant changes observed in IDC tissues without metastasis or with lung metastasis. This further suggests that CD44 and THBS1 may promote specific bone metastasis in IDC. Studies have shown that CD44 can enhance the adhesion of metastatic breast cancer cells to bone marrow endothelial cells [21], consistent with this study's suggestion that increased CD44 expression levels may promote specific bone metastasis in breast cancer.

In other pathways, periostin (POSTN) plays a crucial role in adult skeletal, dental, and cardiac development, as well as tissue repair [22]. POSTN is known to regulate intracellular tyrosine kinase signaling, such as the PI3K-Akt signaling pathway [23]. Increasing evidence indicates that POSTN plays a significant role in breast cancer progression and metastasis. Overexpression of POSTN in human breast cancer cells induces primary tumor growth and angiogenesis in xenograft models by enhancing the expression of vascular endothelial growth factor receptor 2 (VEGFR2) in endothelial cells [24]. In mouse xenograft models, mice with bone metastasis exhibit high POSTN expression in the stroma and plasma surrounding metastatic tumors [25]. POSTN has been identified as a key ECM component of the metastatic niche [26], with studies

suggesting its use as a novel biomarker in combination with CA153 and CEA for breast cancer diagnosis and metastasis prediction [27].

By comparing the differential genes between PyMT-1 with Py-L1 and between PyMT-1 with Py-B1, we found that angiogenesis, ECM-receptor interaction, and the PI3K-Akt signaling pathway were enriched in both GO functional enrichment analysis and KEGG pathway enrichment analysis, suggesting that these cellular activities and pathways may promote both lung and bone metastasis in breast cancer to some extent.

This study conducted transcriptomic sequencing and protein-coding RNA analysis on three cell lines: PyMT-1, Py-L1, and Py-B1. Using GO, KEGG, and GSEA enrichment analyses, we predicted the biological functions of differential genes and performed preliminary validation of some upregulated and downregulated pathway-related genes. By collecting clinical data, we further validated the expression levels of the identified differential genes, gaining a basic understanding of the genetic background of specific lung and bone metastasis in breast cancer. Subsequent research can employ proteomics and metabolomics approaches to more comprehensively investigate the specific mechanisms of breast cancer-specific metastasis, providing a theoretical basis for the clinical treatment of metastatic breast cancer.

This study has several limitations. First, based on the findings of this study, further functional exploration of the important differential genes is indeed necessary, followed by an in-depth investigation of the underlying molecular mechanisms. Second, the breast cancer-specific metastasis model constructed in this study is based on single-cell transcriptomic data, which describes cellular function at the RNA level but does not specifically explore how the identified differential genes and related pathways function in organ-specific metastasis of breast cancer. According to the central dogma of "DNA-RNA-protein, " there is a lack of data on protein expression levels, such as single-cell proteomics data.

## 5. Conclusion

The upregulated enriched pathways among the differential genes between PyMT-1 and Py-L1, such as ECM, focal adhesion, and the PI3K-Akt signaling pathway, may be associated with lung metastasis in breast cancer. The upregulated enriched pathways among the differential genes between PyMT-1 and Py-B1, such as angiogenesis, chemotaxis, positive regulation of cell adhesion, and epithelial cell proliferation, may be associated with bone metastasis in breast cancer.

The expression levels of CCN2 and ITGB6 are elevated in breast cancer tissues with lung metastasis, while the expression levels of CD44 and THBS1 are elevated in breast cancer tissues with bone metastasis.

## Funding

Hebei Health Commission Project (Project No.: 20240287); Hebei Natural Science Foundation of China (Key Program, Project No.: H2024104001).

## Disclosure statement

The authors declare no conflict of interest.

## References


[1] Xia C, Dong X, Li H, et al., 2022, Cancer Statistics in China and the United States, 2022: Profiles, Trends, and Determinants. Chinese Medical Journal, 135(5): 584–590.

[2] Koboldt DC, Fulton RS, McLellan MD, et al., 2012, Comprehensive Molecular Portraits of Human Breast Tumours. Nature, 490(7418): 61–70.

[3] Allemani C, Matsuda T, Di Carlo V, et al., 2018, Global Surveillance of Trends in Cancer Survival 2000–14 (CONCORD-3): Analysis of Individual Records for 37 513 025 Patients Diagnosed with One of 18 Cancers from 322 Population-Based Registries in 71 Countries. The Lancet, 391(10125): 1023–1075.

[4] Zbinden A, Layland SL, Urbanczyk M, et al., 2021, Nidogen-1 Mitigates Ischemia and Promotes Tissue Survival and Regeneration. Advanced Science, 8(4): 2002500.

[5] Wculek SK, Malanchi I., 2015, Neutrophils Support Lung Colonization of Metastasis-Initiating Breast Cancer Cells. Nature, 528(7582): 413–417.

[6] Deepak KGK, Vempati R, Nagaraju GP, et al., 2020, Tumor Microenvironment: Challenges and Opportunities in Targeting Metastasis of Triple Negative Breast Cancer. Pharmacological Research, 153: 104683.

[7] Malanchi I, Santamaria-Martínez A, Susanto E, et al., 2012, Interactions Between Cancer Stem Cells and Their Niche Govern Metastatic Colonization. Nature, 481(7379): 85–89.

[8] Wang Y, Li Y, Zhong J, et al., 2023, Tumor-Derived Cav-1 Promotes Pre-Metastatic Niche Formation and Lung Metastasis in Breast Cancer. Theranostics, 13(5): 1684–1697.

[9] Gao D, Joshi N, Choi H, et al., 2012, Myeloid Progenitor Cells in the Premetastatic Lung Promote Metastases by Inducing Mesenchymal to Epithelial Transition. Cancer Research, 72(6): 1384–1394.

[10] Hongu T, Pein M, Insua-Rodríguez J, et al., 2022, Perivascular Tenascin C Triggers Sequential Activation of Macrophages and Endothelial Cells to Generate a Pro-Metastatic Vascular Niche in the Lungs. Nature Cancer, 3(4): 486–504.

[11] Ghosh P, Dey A, Nandi S, et al., 2025, CTGF (CCN2): A Multifaceted Mediator in Breast Cancer Progression and Therapeutic Targeting. Cancer Metastasis Reviews, 44(1): 32.

[12] Lee SG, Su ZZ, Emdad L, et al., 2008, Astrocyte Elevated Gene-1 Activates Cell Survival Pathways Through PI3K-Akt Signaling. Oncogene, 27(8): 1114–1121.

[13] Gangoda L, Liem M, Ang C, et al., 2017, Proteomic Profiling of Exosomes Secreted by Breast Cancer Cells with Varying Metastatic Potential. PROTEOMICS, 17(23–24): 1600370.

[14] Guise TA., 2013, Breast Cancer Bone Metastases: It's All About the Neighborhood. Cell, 154(5): 957–959.

[15] Ye J, Baer JM, Faget DV, et al., 2024, Senescent CAFs Mediate Immunosuppression and Drive Breast Cancer Progression. Cancer Discovery, 14(7): 1302–1323.

[16] Kiesel L, Kohl A., 2016, Role of the RANK/RANKL Pathway in Breast Cancer. Maturitas, 86: 10–16.

[17] Wan L, Pantel K, Kang Y., 2013, Tumor Metastasis: Moving New Biological Insights into the Clinic. Nature Medicine, 19(11): 1450–1464.

[18] Zhang XHF, Jin X, Malladi S, et al., 2013, Selection of Bone Metastasis Seeds by Mesenchymal Signals in the Primary Tumor Stroma. Cell, 154(5): 1060–1073.

[19] Liang Y, Zhang H, Song X, et al., 2020, Metastatic Heterogeneity of Breast Cancer: Molecular Mechanism and Potential Therapeutic Targets. Seminars in Cancer Biology, 60: 14–27.

[20] Quail DF, Joyce JA, 2013, Microenvironmental Regulation of Tumor Progression and Metastasis. Nature Medicine, 19(11): 1423–1437.

[21] Johnson RW, Finger EC, Olcina MM, et al., 2016, Erratum: Induction of LIFR Confers a Dormancy Phenotype in Breast Cancer Cells Disseminated to the Bone Marrow. Nature Cell Biology, 18(11): 1260–1260.

[22] Balz LM, Bartkowiak K, Andreas A, et al., 2012, The Interplay of HER2/HER3/PI3K and EGFR/HER2/PLC-γ1 Signaling in Breast Cancer Cell Migration and Dissemination. The Journal of Pathology, 227(2): 234–244.

[23] Labrèche C, Cook DP, Abou-Hamad J, et al., 2021, Periostin Gene Expression in Neu-Positive Breast Cancer Cells Is Regulated by a FGFR Signaling Cross Talk with TGFβ/PI3K/AKT Pathways. Breast Cancer Research, 23(1): 107.

[24] Jin L, Han B, Siegel E, et al., 2018, Breast Cancer Lung Metastasis: Molecular Biology and Therapeutic Implications. Cancer Biology & Therapy, 19(10): 858–868.

[25] Morra L, Moch H., 2011, Periostin Expression and Epithelial-Mesenchymal Transition in Cancer: A Review and an Update. Virchows Archiv, 459(5): 465–475.

[26] Lin S, Zhou M, Cheng L, et al., 2024, Exploring the Association of POSTN+ Cancer-Associated Fibroblasts with Triple-Negative Breast Cancer. International Journal of Biological Macromolecules, 268(Pt 1): 131560.

[27] Jia L, Li G, Ma N, et al., 2022, Soluble POSTN Is a Novel Biomarker Complementing CA153 and CEA for Breast Cancer Diagnosis and Metastasis Prediction. BMC Cancer, 22(1): 760.